



## 20 years of ClO measurements in the Antarctic lower stratosphere

Gerald E. Nedoluha<sup>1</sup>, Brian J. Connor<sup>2</sup>, Thomas Mooney<sup>2</sup>, James W. Barrett<sup>3</sup>, Alan Parrish<sup>4</sup>, R. Michael Gomez<sup>1</sup>, Ian Boyd<sup>2</sup>, Douglas R. Allen<sup>1</sup>, Michael Kotkamp<sup>5</sup>, Stefanie Kremser<sup>6</sup>, Terry Deshler<sup>7</sup>, Paul Newman<sup>8</sup>, and Michelle L. Santee<sup>9</sup>

<sup>1</sup>Naval Research Laboratory, Washington, D.C., USA

<sup>2</sup>BC Scientific Consulting LLC, Stony Brook, NY, USA

<sup>3</sup>Stony Brook University, Stony Brook, NY, USA

<sup>4</sup>Department of Astronomy, University of Massachusetts, Amherst, MA, USA

<sup>5</sup>National Institute of Water and Atmospheric Research, Lauder, New Zealand

<sup>6</sup>Bodeker Scientific, Alexandra, New Zealand

<sup>7</sup>Department of Atmospheric Science, University of Wyoming, Laramie, WY, USA

<sup>8</sup>NASA Goddard Space Flight Center, Greenbelt, MD, USA

<sup>9</sup>Jet Propulsion Laboratory, California Institute of Technology, Pasadena, CA, USA

Correspondence to: Gerald E. Nedoluha (nedoluha@nrl.navy.mil)

Received: 2 March 2016 – Published in Atmos. Chem. Phys. Discuss.: 5 April 2016

Revised: 18 July 2016 – Accepted: 30 July 2016 – Published: 30 August 2016

**Abstract.** We present 20 years (1996–2015) of austral springtime measurements of chlorine monoxide (ClO) over Antarctica from the Chlorine Oxide Experiment (ChlOE1) ground-based millimeter wave spectrometer at Scott Base, Antarctica, as well 12 years (2004–2015) of ClO measurements from the Aura Microwave Limb Sounder (MLS). From August onwards we observe a strong increase in lower stratospheric ClO, with a peak column amount usually occurring in early September. From mid-September onwards we observe a strong decrease in ClO. In order to study interannual differences, we focus on a 3-week period from 28 August to 17 September for each year and compare the average column ClO anomalies. These column ClO anomalies are shown to be highly correlated with the average ozone mass deficit for September and October of each year. We also show that anomalies in column ClO are strongly anticorrelated with 30 hPa temperature anomalies, both on a daily and an interannual timescale. Making use of this anticorrelation we calculate the linear dependence of the interannual variations in column ClO on interannual variations in temperature. By making use of this relationship, we can better estimate the underlying trend in the total chlorine ( $\text{Cl}_y = \text{HCl} + \text{ClONO}_2 + \text{HOCl} + 2 \times \text{Cl}_2 + 2 \times \text{Cl}_2\text{O}_2 + \text{ClO} + \text{Cl}$ ). The resultant trends in  $\text{Cl}_y$ , which determine the long-term trend in ClO, are estimated to be  $-0.5 \pm 0.2$ ,

$-1.4 \pm 0.9$ , and  $-0.6 \pm 0.4 \text{ \% year}^{-1}$ , for zonal MLS, Scott Base MLS (both 2004–2015), and ChlOE (1996–2015) respectively. These trends are within  $1\sigma$  of trends in stratospheric  $\text{Cl}_y$  previously found at other latitudes. The decrease in ClO is consistent with the trend expected from regulations enacted under the Montreal Protocol.

### 1 Introduction

Chlorine monoxide (ClO) is central to the formation of the Antarctic ozone hole. It is both the direct product of the reaction between chlorine (Cl) and ozone ( $\text{O}_3$ ) and the catalytic agent in the most important ozone-depleting chemical cycle ( $\text{Cl} + \text{O}_3 \rightarrow \text{ClO} + \text{O}_2$ ;  $\text{ClO} + \text{O} \rightarrow \text{Cl} + \text{O}_2$ ; Waters et al., 1993; Salawitch et al., 1993). Understanding trends in ClO is therefore critical to our understanding of polar ozone recovery. The Antarctic spring is unusual in that, in the lower stratosphere, most of the available total chlorine ( $\text{Cl}_y$ ) is present in its reactive forms ( $\text{ClO}_x = \text{ClO} + 2 \times \text{Cl}_2\text{O}_2$ ). The amount of ClO in the Antarctic vortex is dependent upon both the available  $\text{Cl}_y$  and on the prevalence of polar stratospheric clouds (PSCs), which provide the surfaces for heterogeneous processes that convert unreactive chlorine species into  $\text{ClO}_x$ . While  $\text{Cl}_y$  will vary from year to year due to dy-

namical effects (Strahan et al., 2014), it will vary much less than ClO, which, because of its sensitivity to the prevalence of PSCs, is very sensitive to interannual variations in temperature. The primary goal of this study is to estimate the trend in Cl<sub>y</sub> in the Antarctic lower stratosphere, during the annual formation of the ozone hole, over the period 1996 to 2015.

The ClO molecule has emission lines at microwave frequencies, and the first ground-based measurements of stratospheric ClO were made using a microwave radiometer in 1980 (Parrish et al., 1981). High concentrations of ClO in the lower stratosphere over Antarctica were first measured using this technique in 1986 (de Zafra et al., 1987; Solomon et al., 1987). The Chlorine Oxide Experiment (ChlOE1) ground-based millimeter wave spectrometer was permanently deployed at Scott Base, Antarctica (77.85° S, 166.77° E), by Stony Brook University and the National Institute of Water and Atmospheric Research (NIWA) in February 1996. Details of the measurement technique, data analysis, and error analysis were presented in Solomon et al. (2000). ChlOE1 is currently jointly operated by the Naval Research Laboratory (NRL) and NIWA. Both this instrument and the ChlOE3 instrument, which operated at Mauna Kea, Hawaii, until 2015, are part of the Network for the Detection of Atmospheric Composition Change (NDACC). A new ChlOE4 instrument has now been deployed at Mauna Loa, Hawaii.

In this paper, we describe the measurement technique and present results from the ChlOE1 time series from 1996 to 2015. Measurements are only shown from mid-August to mid-October, when ClO daytime mixing ratios can reach up to ~2 ppbv. We show, from 2004 onwards, ClO measurements from the Aura Microwave Limb Sounder (MLS), both coincident with Scott Base and zonally averaged at the latitude of Scott Base. The ChlOE1 measurements were previously compared with the v1.5 MLS retrievals for the austral spring of 2005 (Connor et al., 2007). Comparisons of measurements taken within ±30 min of the MLS ascending orbit overpass showed agreement of 11 ± 8 % in the peak mixing ratios.

We also show annual anomalies for measurements during the 3 weeks when the stratospheric ClO column densities generally reach their maximum values and compare these anomalies with interannual anomalies in temperature, as provided by the Modern Era Reanalysis for Research and Applications (MERRA) (Rienecker et al., 2011). We use the 20 years of ChlOE measurements and 12 years of MLS measurements to derive a relationship between the interannual anomalies in ClO column and those in 30 hPa temperature. We then make use of this relationship to derive an estimate of Cl<sub>y</sub> trends in the Antarctic vortex.

## 2 ClO measurements

The ChlOE ground-based radiometer measures the thermally excited rotational emission lines near 278.63 GHz. The spec-

trometer bandwidth permits measurement of the pressure-broadened lineshape from which ClO altitude profiles are retrieved. The instrument is a cryogenically cooled (~20 K) heterodyne receiver, tuned to observe the ClO transition by adjustment of a phase-locked local oscillator. It is coupled to a spectrometer with 506 MHz total bandwidth, which is approximately the width of the ClO line at 15 km altitude.

At night, the ClO emission is much weaker and narrower, because nearly all ClO in the lower stratosphere rapidly converts to chlorine peroxide (Cl<sub>2</sub>O<sub>2</sub>) after sunset (Solomon et al., 2002). This allows us, in the ground-based measurements, to remove the instrumental baseline and a small number of interfering atmospheric spectral lines in the instrument bandpass (primarily the ozone line at 278.521 GHz) by subtracting the nighttime spectrum from the daytime one. For these measurements we have defined day as the period from 3 h after sunrise to 1 h before sunset, and night as the period from 4 h after sunset to 1 h before sunrise. Sunrise and sunset are defined to occur when the solar zenith angle is 94.5° at the surface (equivalent to 90° near ~20 km altitude). These day and night variations were chosen empirically, in an attempt to estimate daytime and nighttime equilibrium concentrations of ClO, by excluding times near sunrise and sunset when we observed rapid diurnal changes in ClO. If more observations are included in either daytime or nighttime integrations, these periods of rapid change are partially included, significantly changing the mean values. If fewer observations are included, the integrated spectra are noisier and the mean ClO is correspondingly more uncertain.

A retrieval of the “day minus night” spectrum, and thus of the day ClO mixing ratio less the night mixing ratio, is performed by a three-stage process, described in detail by Solomon et al. (2000). The first stage determines the altitude of the peak of the lower stratospheric distribution as a function of date, by performing retrievals on a full season of data, using an a priori profile without a separate lower stratospheric component. In the second stage, the a priori ClO distribution consists of a climatological profile having a peak in the lower stratosphere determined by stage 1 at ~30 hPa (22 km) in mid-August to ~48 hPa (19 km) by late September, with a secondary peak in the upper stratosphere at ~5 hPa. The second-stage retrieval is simply a nonlinear least-squares fit of a single multiplier applied to the lower stratospheric distribution. The climatological distribution, modified by the retrieved multiplier, is used as the a priori distribution for the third stage, which is a maximum a posteriori solution as given by Rodgers (2000, e.g., Eq. 4.5). Figure 1 shows a ChlOE1 day minus night retrieval for 4 September 2011. The retrieved and a priori profiles both have two mixing ratio peaks, one peak in the upper stratosphere and a much larger peak in the lower stratosphere. The lower stratospheric peak is only present when inactive chlorine is converted to active chlorine on the surface of PSCs and is therefore only observed under the extremely cold Arctic and Antarctic conditions where PSC formation is possi-

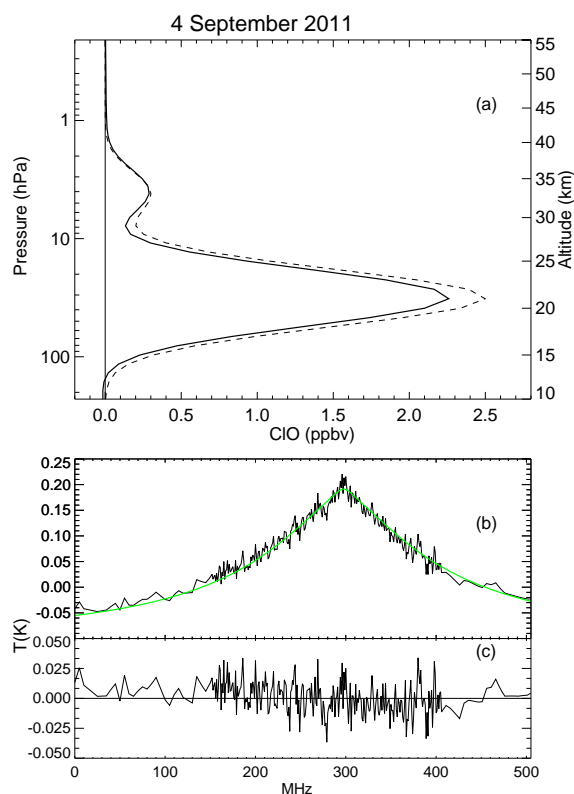


**Figure 1.** (a) The retrieved day minus night ClO mixing ratio profile for 4 September 2011 (solid line), and the a priori profile for that day (dashed line), as a function of pressure (left y axis) and geometric altitude (right y axis). (b) The measured (black line) and modeled (green line) spectra. (c) The measured minus modeled residual spectrum.

ble (temperatures below  $\sim 195$  K). The upper stratospheric ClO peak can be observed at any location, but because of the weak signal, the best ground-based measurements require extended integrations ( $\sim 1$  week) from a high-altitude site. Measurements of this ClO peak, as made from the ChOE3 instrument at Mauna Kea, have been shown in Nedoluha et al. (2011) and Connor et al. (2013). Since all of the measurements shown here are from the ChOE1 instrument, we will henceforth refer to this instrument simply as ChOE.

As is clear in Fig. 1 and has previously been shown by ground-based microwave (de Zafra et al., 1987; Solomon et al., 1987, 2000) and satellite measurements (e.g., Waters et al., 1993; Santee et al., 2005), ClO in the Antarctic spring is overwhelmingly concentrated in the lower stratosphere. We shall, throughout this study, make use of the column ClO at altitudes above 100 hPa. Any variations in this ClO column during the polar PSC season are dominated by changes in the lower stratospheric peak of ClO.

Aura MLS measurements of ClO are available since 2004. The version 2.2 ClO measurements were validated in Santee et al. (2008). Here, we use the v4.2 retrievals (Livesey

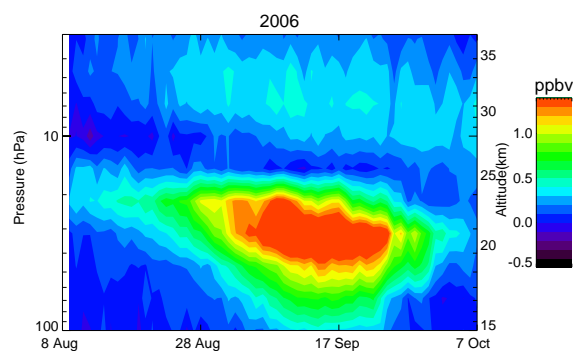


**Figure 2.** The zonally averaged daily ClO mixing ratio (day minus night) as measured by Aura MLS for 2006.

et al., 2016). The Aura measurement overpasses near the latitude of Scott Base occur at  $\sim 16:30$  and  $\sim 23:00$  LST. The times for these measurements remain consistent within  $\pm 4$  min throughout the entire Aura mission. Although it is not possible to replicate the ChOE diurnal sampling with the twice daily MLS overpass sampling, we shall nevertheless in this study show exclusively MLS daytime ( $\sim 16:30$  LST) minus nighttime ( $\sim 23:00$  LST) measurements. We note that at the  $78^\circ$  S latitude of Scott Base the sun actually sets before 16:30 at 23 km (i.e., near the ClO peak) until 24 August.

The typical seasonal evolution of ClO, as measured by MLS, is shown in Fig. 2. This figure shows zonal average day minus night MLS measurements within  $\pm 2^\circ$  latitude of Scott Base for 2006. As in Fig. 1 both the upper and lower stratospheric peaks in ClO are apparent. The ClO begins to increase in the sunlit portions of the vortex in late May/early June as the reservoir gases, hydrogen chloride (HCl) and chlorine nitrate (ClONO<sub>2</sub>), are converted to ClO. The lower-altitude ClO continues to show a gradual increase until mid-September and then experiences a sharp decline, as it converts back to the reservoir gases. Santee et al. (2008) present a detailed study of the seasonal evolution of the partitioning between ClO, HCl (from MLS), and ClONO<sub>2</sub> (from the Atmospheric Chemistry Experiment Fourier Transform Spectrometer; ACE-FTS) in the Arctic and Antarctic.

Figure 3 shows measurements of day minus night ClO column from ChOE during 2006 together with those from the coincident (within  $\pm 2^\circ$  latitude and  $\pm 15^\circ$  longitude of Scott Base) MLS measurements. ChOE measurements are missing for some days because poor tropospheric weather made it impossible to obtain both the daytime and nighttime spectra required for the retrieval, but the general temporal development is clear in both the MLS and ChOE datasets. Essentially there is an increase in August, a maximum in mid-September and then a rapid decrease at the end of winter.

In addition to the daily measurements for 2006, we also plot the ChOE and MLS climatologies for these datasets. The ChOE climatology is calculated from the daily average of all measurements taken from 1996 to 2015, while the MLS

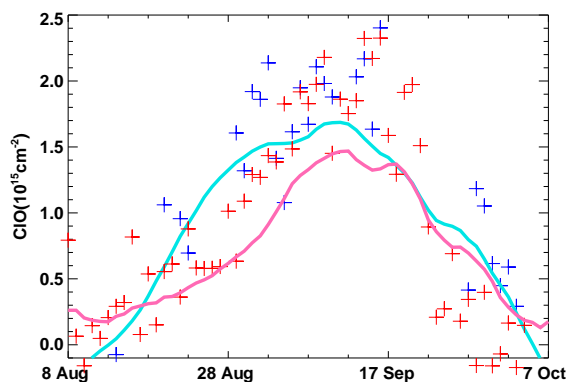


**Figure 3.** Daily (day minus night) column density of ClO measurements at altitudes above 100 hPa for mid-August to mid-October 2006 from ChIOE measurements at Scott Base (blue crosses) and from MLS measurements within  $\pm 2^\circ$  latitude and  $\pm 15^\circ$  longitude of Scott Base (red crosses). Also shown are climatologies for this period based on the ChIOE measurements from 1996 to 2015 (light blue line) and MLS measurements from 2004 to 2015 (pink line).

climatology is derived from measurements taken from 2004 to 2015. Calculating the ChIOE climatology using only measurements from 2004 to 2015 makes very little difference in the analysis. In both cases a 5-day smoothing has been applied. Both datasets show values of the 2006 ClO column that, at least until mid-September, are generally higher than their climatologies. Santee et al. (2011) previously noted that the 2006 Antarctic winter showed strong and prolonged chlorine activation in the lowermost vortex and postulated that this was the cause of unusually low column ozone that year.

Figure 3 shows a clear difference in the seasonal development of the day minus night MLS and ChIOE climatologies. Since the MLS measurements in the vicinity of Scott Base only begin to see sunlit air near the altitude of the ClO peak near 24 August, the fast increase in ClO measured by MLS between 28 August and 7 September is to some extent caused by the very large fractional increase in sunlight exposure during this period. Figure 4 shows the diurnal variation of ChIOE ClO column density for measurements at Scott Base on days when hourly measurements were possible. As is seen in the climatologies in Fig. 3, the difference between the MLS and ChIOE measurements decreases as the length of daylight increases and the 16:30 LST MLS measurement becomes more representative of a mid-day measurement.

We note that Upper Atmosphere Research Satellite (UARS) MLS ClO measurements are available for the years 1991–1993. Using the ground-based ChIOE measurements from Mauna Kea, we previously showed that the UARS MLS ClO measurements in the upper stratosphere were consistent with the Aura MLS ClO measurements (agreeing to within  $\sim 1 \pm 4\%$  ( $2\sigma$ ); Nedoluha et al., 2011). However, unlike Aura MLS, UARS MLS was in a precessing orbit, and therefore the local solar times of measurements varied from day

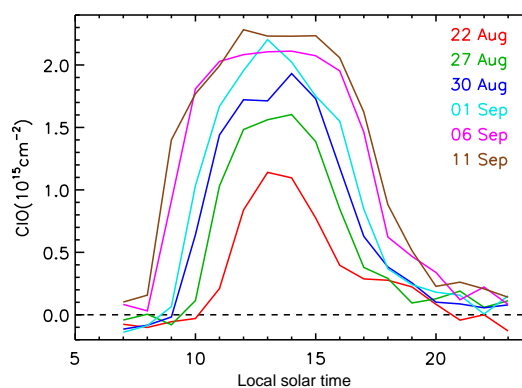


**Figure 4.** The diurnal variation of ClO column density at altitudes above 100 hPa at Scott Base as measured from a series of measurement days in 2005. The date given for each curve is the middle date of a 3-day average of hourly measurements.

to day. Given the large diurnal variability of lower stratospheric ClO in the vortex we would require an extremely accurate model in order to be able to usefully compare the UARS MLS ClO measurements with other measurements in this study.

### 3 Annual ClO anomalies

On the basis of 20 years of springtime lower stratospheric ClO measurements from Scott Base, and 12 years of MLS measurement near this latitude, we will provide an estimate of the trend in  $Cl_y$  in this region which underlies the trend in ClO. To calculate this trend, we need a period over which we have an adequate number of elevated ClO measurements, and during which the year-to-year differences resulting from meteorological variations are minimized. As was shown in Figs. 2 and 3, there is a gradual increase in ClO at the latitude of Scott Base from  $\sim 28$  August to 17 September. At the latitude of Scott Base ( $77.85^\circ$  S), we do not expect that during these dates any of the measurements have occurred outside of the vortex (except possibly in 2002, when the Antarctic stratosphere exhibited an unusual major warming). In the weeks after 17 September, there is generally a very sharp drop in ClO, with the exact timing of this drop differing from year to year. As a measure of this increased variation, we note that the standard deviation of the 12 years of MLS measurements near Scott Base increases from 29 % of the ClO column on 17 September to 58 % of the ClO column on 22 September. We therefore choose 17 September as the final day of the period for which we will compare interannual variations. On 28 August, the climatological ClO from the ChIOE measurements is similar to that on 17 September, and the ChIOE measurements show a steep increase up to this date. The choice of 28 August as the first day for the comparisons provides us a 3-week period with an average of 16.4 daily measurements from ChIOE for each year.

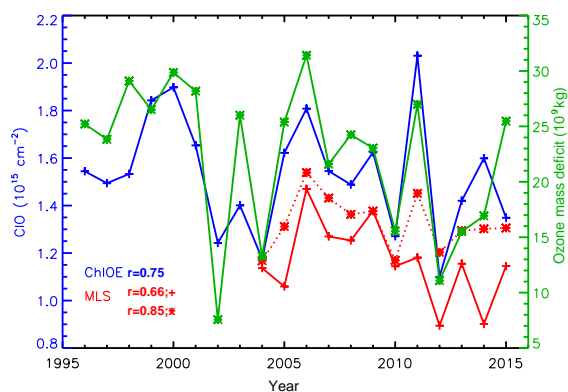


**Figure 5.** The climatology plus annual average anomaly (1) day minus night ClO column density for 28 August to 17 September of each year, calculated as described in text. Averages are shown for ChIOE at Scott Base (blue), MLS coincident with Scott Base (solid red), and MLS at the latitude of Scott Base (dashed red line). Also shown is the ozone mass deficit in  $10^9$  kg of ozone relative to the 220 DU value (green line, with right-hand axis). The correlation coefficients between the ClO measurements and the ozone mass deficit are indicated.

We calculate, for the chosen 3-week period, an annual anomaly for each measurement dataset by taking the average difference from the climatology. We then add back the climatological average column ClO for the period so that we can express changes in ClO both in absolute and in fractional terms. So for each year we plot in Fig. 5

$$Y(\text{year}) = Y_{\text{climo}} + [1/n(\text{year})] \sum [D(\text{year}, \text{day}) - D_{\text{climo}}(\text{day})], \quad (1)$$

where  $Y_{\text{climo}}$  is the dataset-specific climatological average column ClO for the 3-week period,  $n(\text{year})$  is the number of measurement days during that specific year, the sum is over the measurement days,  $D(\text{year}, \text{day})$  is the measured column ClO for that day, and  $D_{\text{climo}}(\text{day})$  is the dataset-specific climatological average column ClO for that day of the year. MLS values are shown both for the zonal average (within  $77.85^\circ \text{S} \pm 2^\circ$ ) and with a further restriction to within  $\pm 15^\circ$  longitude of Scott Base. As expected from the difference in diurnal sampling, the MLS average column day minus night ClO values are somewhat smaller than those from the ChIOE measurements.

We also show in Fig. 5 the average ozone mass deficit (in  $10^9$  kg of ozone relative to the 220 DU value) for September and October of each year. These data were obtained from NASA Ozone Watch (<http://ozonewatch.gsfc.nasa.gov>, Newman, 2016) and are based upon data from the Total Ozone Mapping Spectrometer (TOMS) and the Ozone Monitoring Instrument (OMI), with missing data filled in by the Goddard Earth Observing System Model (GEOS-5).

Figure 5 shows a strong correlation between the annual average ClO column and the ozone mass deficit. For the

20 years of ChIOE measurements the correlation coefficient between these is 0.75. The correlation coefficient increases to 0.78 if we do not include 2014, for which there are only 6 ChIOE measurement days out of a possible 21 between 28 August and 17 September, as opposed to the annual average of 16.4 measurement days. For the 12 years of Aura MLS ClO column measurements, the correlation coefficient is 0.66 for the measurements coincident with Scott Base, and 0.85 for the zonally averaged measurements at the Scott Base latitude.

#### 4 Temperature and ClO

The fraction of  $\text{Cl}_y$  that is in the form of ClO is sensitive to the availability of PSCs, which require low temperatures (below  $\sim 195$  K). As was noted by Santee et al. (2011) for the 2006 winter, the chlorine deactivation and the dissipation of PSCs as observed by the Cloud-Aerosol Lidar and Infrared Pathfinder Satellite Observations (CALIPSO; Pitts et al., 2009) both occur in mid-October. While the variation in ClO measured at any one place and time is dependent not just upon the local temperature but also upon the temperature history of the measured parcel, we do find that in many cases sudden changes in local temperatures coincide with changes in measured ClO. An example of the sensitivity of ClO to changes in temperature is seen very clearly in Fig. 1 of Kremser et al. (2011), where a sudden increase in temperature in early September over Scott Base resulted in a sudden decrease in measured ClO.

Figure 6 shows daily (day minus night) ChIOE column measurements for mid-August to mid-October 2000. This is the same as Fig. 3, but for a different (pre-Aura MLS) year. Also shown in Fig. 6 are MERRA temperatures at 30 hPa (the pressure level nearest to the ClO mixing ratio peak) within  $\pm 2^\circ$  latitude and  $\pm 15^\circ$  longitude of Scott Base. In addition, we show the climatological temperature from the same 20-year time period as the ChIOE measurements. While the temperatures in late August are clearly colder than those in September, the ClO during this period remains low because of a lack of the sunlight required for the activation of chlorine. Once sunlight becomes available, the ClO column begins to increase and, in this particular year, increases to levels well above the climatology. As Fig. 5 shows, this year is second only to 2011 in the annual average ClO column for 28 August to 17 September. At the same time, Fig. 6 shows that the temperatures are colder than the climatology from 28 August to 15 September and are then warmer than the climatology for 6 of the next 7 days. The date when the temperature crosses from below to above the climatological value is the same date on which the ClO column density crosses from above to below the climatology.

The annual average MERRA temperature anomalies at three pressure levels (20, 30, and 40 hPa) are plotted in Fig. 7. As in Fig. 5, these are calculated by taking the average dif-



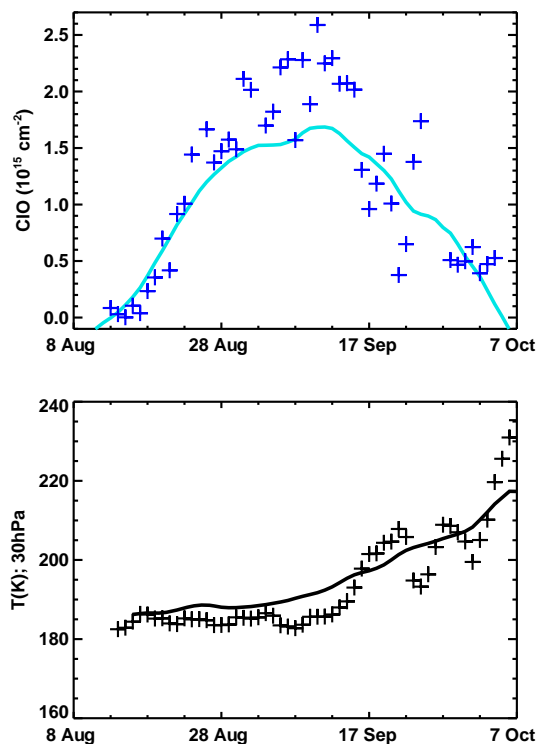


**Figure 6.** Top panel: daily (day minus night) ChIOE1 column density measurements for mid-August to mid-October 2000 (crosses) and a climatology for that period based on the ChIOE measurements from 1996 to 2015 (solid line). Bottom panel: daily 30 hPa temperature from MERRA within  $\pm 2^\circ$  latitude and  $\pm 15^\circ$  longitude of Scott Base (crosses) and a 1996–2015 climatology for this location (solid line).

ference between the daily temperature and the temperature climatology for that day over the 3-week period of 28 August to 17 September, but here we do not add back the climatological temperature average. We find that the relationship between temperatures at these three levels changed between 1998 and 1999. The 20 and 30 hPa temperature anomalies suggested extremely cold years from 1996 to 1998 (at 20 hPa 1996 and 1997 were the coldest years), while at 40 hPa none of these three years was the coldest in the 20-year record.

In between the 1998 and 1999 periods that we analyzed, data from the Advanced TIROS (Television Infrared Observation Satellite) Operational Vertical Sounder (ATOVS, on NOAA15) began to be assimilated into the MERRA analysis, and it has been shown that this causes some inhomogeneities in the reanalysis (Pawson, 2012). We therefore compared the MERRA temperatures with sondes launched from Scott Base from 1996 to 1998, and with sondes launched from 1999 to 2010. We found that the cold bias of MERRA relative to the sondes at 20 hPa was much reduced in the 1999–2010 MERRA temperatures. Due to the biases in MERRA temperatures indicated by the sonde data, we added 4.0 K to the 20 hPa 1996–1998 MERRA temperatures and 2.1 K to the

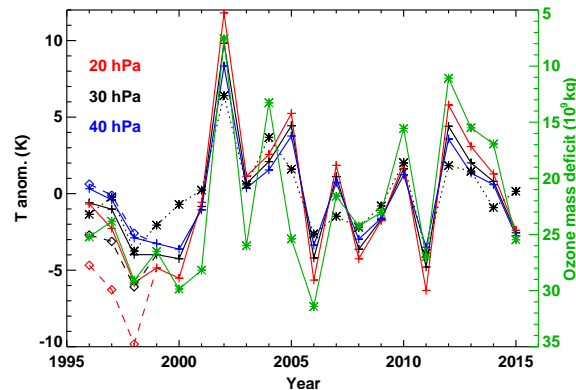


**Figure 7.** Annual average temperature anomalies for 28 August to 17 September within  $\pm 2^\circ$  latitude and  $\pm 15^\circ$  longitude of Scott Base. Results are shown at 20 (red), 30 (black), and 40 hPa (blue). The dashed lines for 1996–1998 show the anomalies before applying the bias correction to the MERRA temperatures (see text). Also shown (dotted black line) is the zonal temperature anomaly for this latitude range. The green line shows the ozone mass deficit, with values given on the right-hand axis (as in Fig. 5, but with the axis reversed).

30 hPa temperatures to account for this temperature bias. We also subtracted 0.3 K from the 40 hPa 1996–1998 MERRA temperatures. When we estimate chlorine trends in Sect. 5, it will be particularly important to have temperatures during these first three years of ChIOE measurements that are consistent with temperatures in later years.

Given the anti-correlation between column ClO and temperature, we would expect an anti-correlation between temperature and ozone loss. Just as in Fig. 5, we therefore also show in Fig. 7 the ozone mass deficit, although in this case with the scale inverted. The magnitude of the anti-correlation between the 30 hPa temperature anomalies over Scott Base and the ozone mass deficit shown in Fig. 7 is comparable to that of the correlation between ClO and ozone mass deficit shown in Fig. 5, with a correlation coefficient of  $-0.82$ , while for the zonal average temperatures the correlation drops to  $-0.78$ . The temperature and ozone mass deficit have a slightly weaker correlation at 40 hPa, while at 20 hPa the correlation is slightly stronger for the local temperatures and slightly weaker for the zonal average temperatures.

Figure 8 presents scatter plots of the annual average column ClO and the 30 hPa temperature anomalies for 28 August to 17 September. Since, after the bias correction, the temperature anomalies are very similar for all three pressure levels, the anomalies shown in Fig. 8 are nearly independent of the pressure level chosen for the temperatures. We chose 30 hPa since, among the three pressure levels shown in Fig. 7, zonally averaged temperatures at this level showed the highest correlation with MLS zonally averaged column ClO measurements (correlation coefficients of  $-0.862$ ,  $-0.863$ , and  $-0.781$  at 20, 30, and 40 hPa respectively). For the local

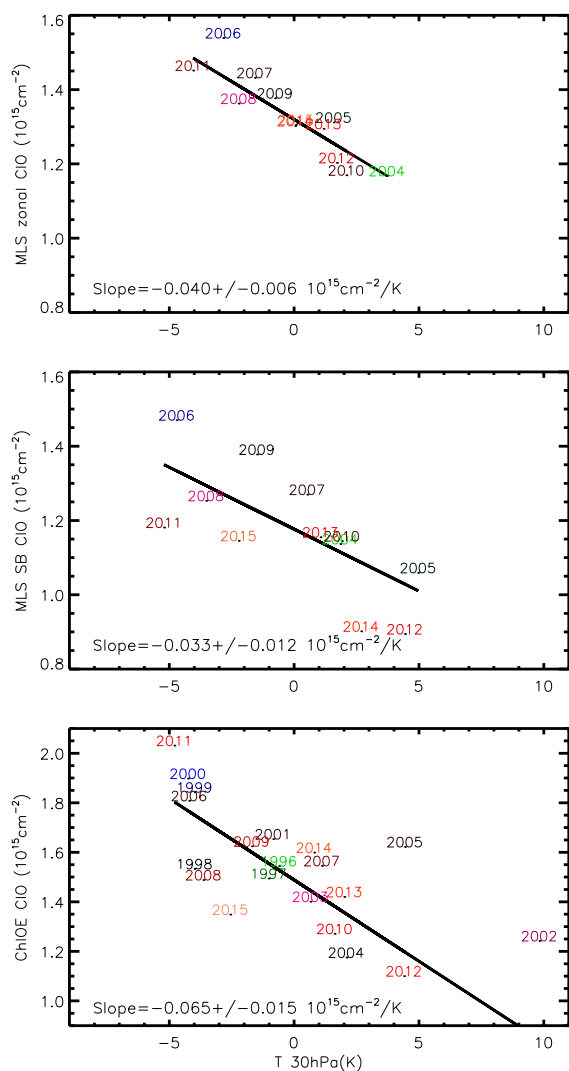


**Figure 8.** The climatology plus annual average anomaly for the 28 August to 17 September column ClO (shown in Fig. 5) plotted against the temperature anomalies (shown in Fig. 7). Also shown are linear fits with a  $1\sigma$  error estimate. Results are shown for the zonally average MLS ClO column measurements and 30 hPa MERRA temperatures within  $\pm 2^\circ$  latitude of Scott Base (top), for MLS ClO and MERRA temperatures with a further restriction to within  $\pm 15^\circ$  longitude of Scott Base (middle), and for ChIOE ClO measurements and MERRA temperatures with this tighter restriction (bottom).

MLS measurements and ChIOE, the correlation with local temperatures was slightly higher at 20 hPa. Results are shown for ChIOE measurements, as well as for MLS measurements both zonally averaged (with corresponding zonally averaged temperatures) and restricted to within  $\pm 2^\circ$  latitude and  $\pm 15^\circ$  longitude of Scott Base.

To establish a linear fit for the annual average anomalies shown in Fig. 8, we need to estimate uncertainties in the temperature and ClO measurements. We estimate these uncertainties by calculating the standard error of the mean for the

daily anomalies for each year. This will tend to weight years that have consistently high (or low) ClO column and temperature anomalies, as well as, for ChIOE, years when there are a large number of measurements (MLS almost always has measurements for every day). The uncertainties for each year are generally similar, but in 2014 there were very few ChIOE measurements and these measurements were particularly variable.

We calculated linear fits and found that the slopes were  $-0.040 \pm 0.006 \times 10^{15}$ ,  $-0.033 \pm 0.012 \times 10^{15}$ , and  $-0.065 \pm 0.015 \times 10^{15} \text{ cm}^{-2} \text{ K}^{-1}$  for the zonal MLS, Scott Base MLS, and ChIOE ClO measurements, respectively. We attribute the difference in the linear fits between the ChIOE and MLS ClO measurements to the different diurnal sampling of the ChIOE and MLS measurements. The slopes for the MLS measurements near Scott Base and for the zonally averaged MLS measurements at this latitude are not statistically different.

As a consistency check, we repeated this study using temperatures from the NCEP Reanalysis (REAN2) (Kistler et al., 2001) and calculated fits that were nearly identical to those shown in Fig. 8. The slopes were very close to those calculated with MERRA:  $-0.040 \pm 0.006 \times 10^{15}$ ,  $-0.032 \pm 0.012$ , and  $-0.068 \pm 0.015 \times 10^{15} \text{ cm}^{-2} \text{ K}^{-1}$  for the zonal MLS, Scott Base MLS, and ChIOE ClO measurements, respectively.

## 5 Estimating a chlorine trend

There have been a number of studies attempting to quantify the temporal trend in  $\text{Cl}_y$  using measurements of either HCl or ClO. HCl is the primary reservoir species for chlorine, and measurements of HCl in the upper stratosphere show a decline since around 1997 (Anderson et al., 2000; Froidevaux et al., 2006; Jones et al., 2011; Nedoluha et al., 2011). Jones et al. (2011) showed, for a range of latitude bands, a decrease in HCl measured by the Halogen Occultation Experiment (HALOE) of between 0.4 and 0.6 %  $\text{year}^{-1}$  from 1997 to 2005. Froidevaux et al. (2006) estimated a decrease of  $\sim 0.8 \pm 0.1 \text{ % year}^{-1}$  from Aura MLS HCl measurements over a very brief August 2004 to January 2006 period, but unfortunately the MLS channel measuring HCl near the stratopause experienced rapid deterioration so no extended HCl trend study from the MLS dataset has been possible. Jones et al. (2011) produced a combined ODIN/SMR and MLS ClO dataset for 2001–2008 and calculated a trend of  $-0.7 \pm 0.8 \text{ % year}^{-1}$  ( $2\sigma$ ) in tropical ClO from 35 to 45 km. Nedoluha et al. (2011) used ground-based measurements of ClO from Mauna Kea to show a clear decrease since 1996 and validated the relative consistency of the UARS MLS (1991–1998) and Aura MLS (2004–present) ClO measurements. Finally, Connor et al. (2013) used a reanalyzed version of the ground-based ClO measurements from Mauna

Kea and calculated a trend of  $-0.64 \pm 0.15 \text{ \% year}^{-1}$  ( $2\sigma$ ) from 1995 to 2012.

The linear trend in the annual average ChIOE ClO columns from 28 August to 17 September (those shown in Fig. 5 from 1996 to 2015) is  $-1.1 \pm 0.4 \text{ \% year}^{-1}$ . However, since the first ChIOE measurement years were colder than average, this trend is almost certainly to some extent the result of increased processing on PSC particles during these years and is therefore not representative of the trend in  $\text{Cl}_y$ . In addition, interannual variations in dynamics will cause interannual variations in  $\text{Cl}_y$  which will in turn affect the measured ClO. Strahan et al. (2014) used the compact relationship between nitrous oxide ( $\text{N}_2\text{O}$ ) and  $\text{Cl}_y$ , as established by Schauffler et al. (2003), to estimate the variability in Antarctic  $\text{Cl}_y$  for the years 2004–2012 based upon MLS measurements of  $\text{N}_2\text{O}$ . They found year-to-year variations of  $\text{Cl}_y$  in the vortex on the 500 K potential temperature surface of as much as  $\sim 7 \text{ \%}$ .

Accounting for the dynamical variations over the entire 20-year ChIOE measurement dataset is problematic, and we will not attempt to do so here, but it is certainly possible to account for the interannual temperature variations over this period. Making use of the annual temperature anomalies, we calculate an adjusted annual column ClO, which is given for each year by  $\text{ClO}_{\text{adj}}(\text{year}) = \text{ClO}(\text{year}) - \alpha \Delta T(\text{year})$ , where  $\alpha$  is the temperature dependence of ClO shown in Fig. 8 and  $\Delta T(\text{year})$  is the temperature anomaly for that year. To the extent that we have successfully removed the effect of temperature variations, the variations in the adjusted ClO columns should better represent the variation in  $\text{Cl}_y$ .

The column ClO values, adjusted for interannual temperature variations, are shown in Fig. 9. We then calculate a linear trend using these modified column ClO values and express the trends as a function of the average column values. The resultant trends calculated for zonal MLS, Scott Base MLS (2004–2015), and ChIOE (1996–2015) are  $-0.5 \pm 0.2$ ,  $-1.4 \pm 0.9$ , and  $-0.6 \pm 0.4 \text{ \% year}^{-1}$ , respectively. Note that the  $1\sigma$  error bars shown in this plot are the same as the error estimates used in establishing the ClO column vs. temperature relationship in Fig. 8. The fraction of points falling within  $1\sigma$  of the trend line is approximately what would be expected given a Gaussian distribution, so our uncertainty estimate seems reasonable. If we use the REAN2 temperatures both to establish the relationship between temperature and ClO column and subsequently to calculate trends, then we find trends almost identical to those found with the MERRA temperatures. The calculated trends in adjusted ClO column, as calculated using REAN2 temperatures, are  $-0.6 \pm 0.2$ ,  $-1.4 \pm 0.9$ , and  $-0.5 \pm 0.4 \text{ \% year}^{-1}$  for zonal MLS, Scott Base MLS, and ChIOE, respectively.

While the trends are almost insensitive to the choice of temperature dataset, they are somewhat sensitive to the precise choice of dates from which the annual average is determined. Although we believe that we have made an optimal choice for these dates, it is nevertheless instructive to exam-

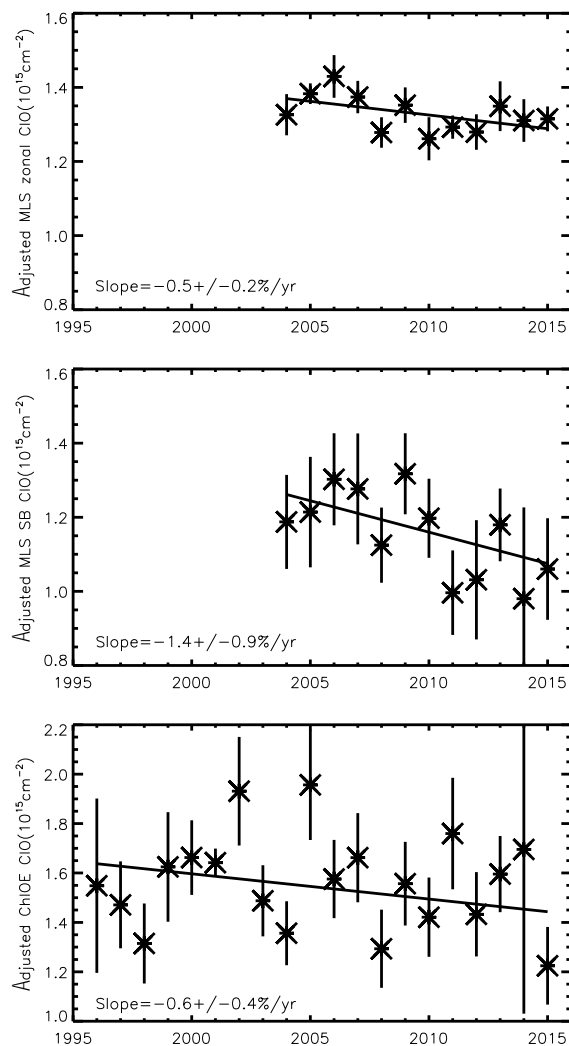


**Figure 9.** The annual average temperature-adjusted ClO columns (see text) for 28 August to 17 September. The adjustment is based upon the annual average temperature and the relationship shown in Fig. 8 (see text). Results are shown for the zonally averaged MLS measurements within  $\pm 2^\circ$  latitude of Scott Base (top), for MLS measurements within  $\pm 2^\circ$  latitude and  $\pm 15^\circ$  longitude of Scott Base (middle), and for ChIOE measurements at Scott Base (bottom). Also shown is a linear fit to the data. Uncertainties are  $1\sigma$ .

ine this sensitivity. If we add or subtract 5 days from the beginning or end of the comparison periods and repeat our calculations for these four additional cases, we find trends in adjusted ClO columns in the range of  $-0.3$  to  $-0.6 \text{ \% year}^{-1}$  for the zonal MLS measurements,  $-0.9$  to  $-1.8 \text{ \% year}^{-1}$  for the local MLS measurements, and  $-0.2$  to  $-0.7 \text{ \% year}^{-1}$  for the ChIOE measurements.

Finally, we have also performed the entire analysis using daytime zonal average MLS measurements without subtracting the nighttime measurements. The results are very similar to the results from day minus night measurements, agreeing



to within  $1\sigma$  in both the sensitivity of the ClO column to temperature, and in the calculated trend.

## 6 Summary

We have shown column ClO from 20 years of ChIOE measurements over Scott Base, Antarctica, as well as from 12 years of Aura MLS measurements near Scott Base and zonally averaged around  $78^\circ\text{S}$ . Interannual variations in column ClO over the 3-week period from 28 August to 17 September were correlated with the average ozone mass deficit for September and October ( $r = 0.75$  for ChIOE). Such a correlation is to be expected, given that ClO is the catalytic agent in the most important ozone-destroying cycle.

We have also shown that the interannual variation in column ClO is anti-correlated with interannual variations in 30 hPa temperature. This is physically reasonable since colder temperatures increase the availability of polar stratospheric clouds, and these will in turn provide the heterogeneous surfaces for the production of ClO (Molina and Molina, 1987; Solomon, 1999).

The multi-year ChIOE and Aura MLS datasets provided the opportunity to study trends. While there have been a number of studies of trends in  $\text{Cl}_y$ , this is to our knowledge the first study that addresses the question of stratospheric  $\text{Cl}_y$  trends in the Antarctic region. Since the ozone hole represents the most extreme manifestation of ozone depletion, it is of particular interest to determine whether the trends in Antarctic stratospheric  $\text{Cl}_y$ , which underlie the trends in ClO that causes this destruction, are similar to those measured elsewhere.

Because of the strong dependence of ClO on temperature, any calculated trend in ClO could misrepresent the trend in  $\text{Cl}_y$ , particularly if there were unusually warm or cold temperatures near the beginning or end of the time series. We therefore used the calculated relationship between interannual variations in column ClO and 30 hPa temperature to account for the effect of variations in column ClO caused by changes in temperature. We then calculated trends in temperature-adjusted ClO. The resultant trends for zonal MLS, Scott Base MLS (2004–2015), and ChIOE (1996–2015) were  $-0.5 \pm 0.2$ ,  $-1.4 \pm 0.9$ , and  $-0.6 \pm 0.4 \text{ \% year}^{-1}$ , respectively. While our temperature regression does not account for dynamical effects that might influence ClO trends (e.g., changes in the Brewer–Dobson circulation), these trends are within  $1\sigma$  of trends in  $\text{Cl}_y$  previously found at other latitudes (WMO, 2014). The decrease in ClO is consistent with the trend expected from regulations enacted under the Montreal Protocol.

## 7 Data availability

The ChIOE data are available from the NDACC data server at <http://www.ndsc.ncep.noaa.gov/data> (NOAA, 2015). MLS

data are available from the NASA Goddard Earth Science Data Information and Services Center (<http://acdisc.gsfc.nasa.gov>, NASA, 2015b). Ozone mass deficit data are available from NASA Ozone Watch (<http://ozonewatch.gsfc.nasa.gov>, NASA, 2015a).

*Acknowledgements.* This project was funded by NASA under the Upper Atmosphere Research Program, by the Naval Research Laboratory, and by the Office of Naval Research. We would like to acknowledge the many Antarctica New Zealand technicians who have supported the daily operation of ChIOE over two decades of measurements. We also acknowledge the logistical support that Antarctica New Zealand has supplied over this period. Work at the Jet Propulsion Laboratory, California Institute of Technology, was carried out under a contract with the National Aeronautics and Space Administration. Sonde temperature data were collected under support from the National Science Foundation.

The data used in this publication were obtained as part of the Network for the Detection of Atmospheric Composition Change (NDACC) and are publicly available (see <http://www.ndacc.org>).

Edited by: G. Brasseur

Reviewed by: two anonymous referees

## References

- Anderson, J., Russell III, J. M., Solomon, S., and Deaver, L. E.: Halogen Occultation Experiment confirmation of stratospheric chlorine decreases in accordance with the Montreal Protocol, *J. Geophys. Res.*, 105, 4483–4490, 2000.
- Connor, B. J., Mooney, T., Barrett, J., Solomon, P., Parrish, A., and Santee, M.: Comparison of ClO measurements from the Aura Microwave Limb Sounder to ground-based microwave measurements at Scott Base, Antarctica, in spring 2005, *J. Geophys. Res.*, 112, D24S42, doi:10.1029/2007JD008792, 2007.
- Connor, B. J., Mooney, T., Nedoluha, G. E., Barrett, J. W., Parrish, A., Koda, J., Santee, M. L., and Gomez, R. M.: Re-analysis of ground-based microwave ClO measurements from Mauna Kea, 1992 to early 2012, *Atmos. Chem. Phys.*, 13, 8643–8650, doi:10.5194/acp-13-8643-2013, 2013.
- de Zafra, R. L., Jaramillo, M., Parrish, A., Solomon, P., Connor, B., and Barrett, J.: High concentrations of chlorine monoxide at low altitudes in the Antarctic spring stratosphere: Diurnal variation, *Nature*, 328, 408–411, 1987.
- Froidevaux, L., Livesey, N. J., Read, W. G., Salawitch, R. J., Waters, J. W., Drouin, B., MacKenzie, I. A., Pumphrey, H. C., Bernath, P., Boone, C., Nassar, R., Montzka, S., Elkins, J., Cunnold, D., and Waugh, D.: Temporal decrease in upper atmospheric chlorine, *Geophys. Res. Lett.*, 33, L23812, doi:10.1029/2006GL027600, 2006.
- Jones, A., Urban, J., Murtagh, D. P., Sanchez, C., Walker, K. A., Livesey, N. J., Froidevaux, L., and Santee, M. L.: Analysis of HCl and ClO time series in the upper stratosphere using satellite data sets, *Atmos. Chem. Phys.*, 11, 5321–5333, doi:10.5194/acp-11-5321-2011, 2011.
- Kistler, R., Kalnay, E., Collis, W., Saha, S., White, G., Woolewn, J., Chelliah, M., Ebisuzaki, W., Kanamitsu, M., Kousky, V., van

- den Dool, H., Jenne, R., and Fiorino, M.: The NCEP-NCAR 50-year reanalysis: Monthly means CDROM and documentation, *B. Am. Meteorol. Soc.*, 82, 247–267, 2001.
- Kremser, S., Schofield, R., Bodeker, G. E., Connor, B. J., Rex, M., Barret, J., Mooney, T., Salawitch, R. J., Canty, T., Frieler, K., Chipperfield, M. P., Langematz, U., and Feng, W.: Retrievals of chlorine chemistry kinetic parameters from Antarctic ClO microwave radiometer measurements, *Atmos. Chem. Phys.*, 11, 5183–5193, doi:10.5194/acp-11-5183-2011, 2011.
- Livesey, N. J., Read, W. G., Wagner, P. A., Froidevaux, L., Lambert, A., Manney, G. Lo, Valle, L. F. M., Pumphrey, H. C., Santee, M. L., Schwartz, M. J., Wang, S., Fuller, R. A., Jarnot, R. F., Knosp, B. W., and Martinez, E.: Version 4.2x Level 2 data quality and description document, Tech. Rep. JPL D-33509 Rev. A, Jet Propulsion Laboratory, available at: <http://mls.jpl.nasa.gov>, last access: 9 May 2016.
- Molina, L. T. and Molina, M. J.: Production of Cl<sub>2</sub>O<sub>2</sub> from the self-reaction of the ClO radical, *J. Phys. Chem.*, 91, 433–436, doi:10.1021/j100286a035, 1987.
- Nedoluha, G. E., Connor, B. J., Barrett, J., Mooney, T., Parrish, A., Boyd, I., Wrotny, J. E., Gomez, R. M., Koda, J., Santee, M. L., and Froidevaux, L.: Ground-based measurements of ClO from Mauna Kea and intercomparisons with Aura and UARS MLS, *J. Geophys. Res.*, 116, D02307, doi:10.1029/2010JD014732, 2011.
- NASA: Ozone Hole Watch, <http://ozonewatch.gsfc.nasa.gov/>, 2015a.
- NASA: MLS data, <http://acdisc.gesdisc.eosdis.nasa.gov/data/>, 2015b.
- NOAA: NDACC Data, <http://www.ndsc.ncep.noaa.gov/data/>, 2015.
- Parrish, A., de Zafra, R. L., Solomon, P. M., Barrett, J. W., and Carlson, E. R.: Chlorine Oxide in the Stratospheric Ozone Layer: Ground-Based Detection and Measurements, *Science*, 211, 1158–1160, 1981.
- Pawson, S.: Representation of the Middle-to-Upper Stratosphere in MERRA, Global Modeling and Assimilation Office Annual Report & Research Highlights, NASA Goddard Space Flight Center, Greenbelt, Maryland, USA, 42–43, 2012.
- Pitts, M. C., Poole, L. R., and Thomason, L. W.: CALIPSO polar stratospheric cloud observations: second-generation detection algorithm and composition discrimination, *Atmos. Chem. Phys.*, 9, 7577–7589, doi:10.5194/acp-9-7577-2009, 2009.
- Rienecker, M. M., Suarez, M. J., Gelaro, R., Todling, R., Bacmeister, J., Liu, E., Bosilovich, M. G., Schubert, S. D., Takacs, L., Kim, G. K., Bloom, S., Chen, J. Y., Collins, D., Conaty, A., Da Silva, A., Gu, W., Joiner, J., Koster, R. D., Lucchesi, R., Molod, A., Owens, T., Pawson, S., Pegion, P., Redder, C. R., Reichle, R., Robertson, F. R., Ruddick, A. G., Sienkiewicz, M., and Woolen, J.: MERRA: NASA's Modern Era Retrospective Analysis for Research and Applications, *J. Climate*, 24, 3624–3648, 2011.
- Rodgers, C. D.: Inverse Methods for Atmospheric Sounding, World Scientific Publishing Co., Hackensack, NJ, 2000.
- Salawitch, R. J., Wofsy, S. C., Gottlieb, E. W., Lait, L. R., Newman, P. A., Schoeberl, M. R., Loewenstein, M., Podolske, J. R., Strahan, S. E., Proffitt, M. H., Webster, C. R., May, R. D., Fahey, D. W., Baumgardner, D., Dye, J. E., Wilson, J. C., Kelly, K. K., Elkins, J. W., Chan, K. R., and Anderson, J. G.: Chemical loss of ozone in the Arctic polar vortex in the winter of 1991–1992, *Science*, 261, 1146–1149, 1993.
- Santee, M. L., Manney, G. L., Livesey, N. J., Froidevaux, L., MacKenzie, I. A., Pumphrey, H. C., Read, W. G., Schwartz, M. J., Waters, J. W., and Harwood, R. S.: Polar processing and development of the 2004 Antarctic ozone hole: First results from MLS on Aura, *Geophys. Res. Lett.*, 32, L12817, doi:10.1029/2005GL022582, 2005.
- Santee, M. L., Lambert, A., Read, W. G., Livesey, N. J., Manney, G. L., Cofield, R. E., Cuddy, D. T., Daffer, W. H., Drouin, B. J., Froidevaux, L., Fuller, R. A., Jarnot, R. F., Knosp, B. W., Perun, V. S., Snyder, W. V., Stek, P. C., Thurstans, R. P., Wagner, P. A., Water, J. W., Connor, B., Urban, J., Murtagh, D., Ricaud, P., Barret, B., Kleinboehl, A., Kuttippurath, J., Kullman, H., von Hobe, M., Toon, G. C., and Stachnik, R. A.: Validation of the Aura Microwave Limb Sounder ClO measurements, *J. Geophys. Res.*, 113, D15S22, doi:10.1029/2007JD008762, 2008.
- Santee, M. L., Manney, G. L., Livesey, N. J., Froidevaux, L., Schwartz, M. J., and Read, W. G.: Trace gas evolution in the lowermost stratosphere from Aura Microwave Limb Sounder measurements, *J. Geophys. Res.*, 116, D18306, doi:10.1029/2011JD015590, 2011.
- Schauffler, S. M., Atlas, E. L., Donnelly, S. G., Andrews, A., Montzka, S. A., Elkins, J. W., Hurst, D. F., Romashkin, P. A., Dutton, G. S., and Stroud, V.: Chlorine budget and partitioning during the Stratospheric Aerosol and Gas Experiment (SAGE) III Ozone Loss and Validation Experiment (SOLVE), *J. Geophys. Res.*, 108, 4173, doi:10.1029/2001JD002040, 2003.
- Solomon, P., Barrett, J., Connor, B. J., Zoonematkermani, S., Parrish, A., Lee, A. M., Pyle, J. A., and Chipperfield, M. P.: Seasonal observations of chlorine monoxide in the stratosphere over Antarctica during the 1996–1998 ozone holes and comparison with the SLIMCAT 3D model, *J. Geophys. Res.*, 105, 28979–29001, 2000.
- Solomon, P., Connor, B., Barrett, J., Mooney, T., Lee, A., and Parrish, A.: Measurements of stratospheric ClO over Antarctica in 1996–2000 and implications for ClO dimer chemistry, *Geophys. Res. Lett.*, 29, 3.1–3.4, doi:10.1029/2002GL015232, 2002.
- Solomon, P. M., Connor, B., de Zafra, R. L., Parrish, A., Barrett, J., and Jaramillo, M.: High concentrations of chlorine monoxide at low altitudes in the Antarctic spring stratosphere: Secular variation, *Nature*, 328, 411–413, 1987.
- Solomon, S.: Stratospheric ozone depletion, A review of concepts and history, *Rev. Geophys.*, 37, 275–316, 1999.
- Strahan, S. E., Douglass, A. R., Newman, P. A., and Steenrod, S. D.: Inorganic chlorine variability in the Antarctic vortex and implications for ozone recovery, *J. Geophys. Res.-Atmos.*, 119, 14098–14109, doi:10.1002/2014JD022295, 2014.
- Waters, J. W., Froidevaux, L., Read, W. G., Manney, G. L., Elson, L. S., Flower, D. A., Jarnot, R. F., and Harwood, R. S.: Stratospheric ClO and ozone from the Microwave Limb Sounder on the Upper Atmospheric Research Satellite, *Nature*, 362, 597–602, 1993.
- WMO (World Meteorological Organization): Scientific Assessment of Ozone Depletion: 2014, World Meteorological Organization, Global Ozone Research and Monitoring Project-Report No. 55, 416 pp., Geneva, Switzerland, 2014.